



NIH PUBLIC ACCESS

## Author Manuscript

*Dev Dyn.* Author manuscript; available in PMC 2011 October 1.

Published in final edited form as:

*Dev Dyn.* 2010 October ; 239(10): 2603–2618. doi:10.1002/dvdy.22393.

## Essential genes for astroglial development and axon pathfinding during zebrafish embryogenesis

**Michael J.F. Barresi<sup>1,\*</sup>, Sean Burton<sup>1,2</sup>, Kristina DiPietrantonio<sup>1</sup>, Adam Amsterdam<sup>3</sup>, Nancy Hopkins<sup>3</sup>, and Rolf O. Karlstrom<sup>2</sup>**<sup>1</sup>Biological Sciences, Smith College, Northampton, MA, 01063<sup>2</sup>Department of Biology, University of Massachusetts, Amherst, MA, 01003<sup>3</sup>Center for Cancer Research and Department of Biology, Massachusetts Institute of Technology, Cambridge, MA 02139

### Abstract

The formation of the central nervous system depends on the coordinated development of neural and glial cell types that arise from a common precursor. Using an existing group of zebrafish mutants generated by viral insertion, we performed a “shelf-screen” to identify genes necessary for astroglial development and axon scaffold formation. We screened 274 of 315 viral insertion lines using antibodies that label axons (anti-Acetylated Tubulin) and astroglia (anti-Gfap) and identified 25 mutants with defects in gliogenesis, glial patterning, neurogenesis, and axon guidance. We also identified a novel class of mutants affecting radial glial cell numbers. Defects in astroglial patterning were always associated with axon defects, supporting an important role for axon-glial interactions during axon scaffold development. The genes disrupted in these viral lines have all been identified, providing a powerful new resource for the study of axon guidance, glio- and neurogenesis, and neuron-glial interactions during development of the vertebrate CNS.

### Keywords

zebrafish; insertional mutants; axon guidance; astroglia; radial glia; glia; POC; chiasm; motor axon; hindbrain; neurogenesis; gliogenesis; Gfap

### Introduction

In the vertebrate central nervous system (CNS) astroglial cells play important roles in synapse formation and maintenance, communication with other glia and neurons, and serve as stem cells that possess both gliogenic and neurogenic properties (Taber and Hurley, 2008). During CNS development, neuroepithelial cells give rise to both neurons and radial glial cells (Tawk et al., 2007). Radial glia possess a unique bipolar morphology, with the shorter of the two processes contacting the ventricular zone of the CNS and the longer process extending to the pial surface (Chanas-Sacre et al., 2000). These radial glia function as stem cells to generate more neurons and glia (Raymond et al., 2006; Bernardos et al., 2007; Kim et al., 2008; Kriegstein and Alvarez-Buylla, 2009; Lam et al., 2009). Astrocytes and oligodendrocytes are two glial subtypes that differentiate from radial glia (reviewed in (Campbell and Gotz, 2002)). In zebrafish, radial glial cells have recently been shown to give rise to oligodendrocytes in the developing spinal cord that later function to myelinate axons of the CNS (Kim et al., 2008; Lam et al., 2009). Astrocytes, while morphologically distinct

\*Corresponding author: [mbarresi@email.smith.edu](mailto:mbarresi@email.smith.edu); ph. 413.585.3697; fax. 413.585.3786.

from radial glia, exhibit some of the same molecular characteristics, including the expression of the Glial fibrillary acidic protein (Gfap). Due to the molecular and lineage similarities various astrocytes and their progenitor cells are all collectively referred to as astroglia (Campbell and Gotz, 2002; Taber and Hurley, 2008).

After an initial phase of neurogenesis and gliogenesis, neurons extend axons in search of their synaptic targets. Gfap expressing glia differentiate prior to the formation of an early axon scaffold and these glial cells are known to provide important cues that guide migrating neurons and axons (Learte and Hidalgo, 2007). In *Drosophila*, midline glia provide a growth substrate for growing axons and produce many key guidance cues that either attract or repel commissural axons at the midline (Kaprielian et al., 2001). In both mouse and zebrafish, radial glia and other astroglia are associated with formation of the forebrain commissures and the optic chiasm (Marcus and Easter, 1995; Shu et al., 2003a; Shu et al., 2003b; Barresi et al., 2005), although the mechanistic role for glia in axon scaffold formation has yet to be determined.

Since Ramón y Cajal first observed the intimate association between neurons and glia in the vertebrate CNS it has been clear that interactions of these cell types is likely to be critical for both the development and function of nervous systems (Ramón y Cajal, 1911; Shaham, 2005). It is now clear that glia play a central role in the formation of the CNS, including neurogenesis, neural patterning, axon scaffolding, synapse formation, the formation of the blood-brain barrier, and even regeneration (Powell et al., 1997; Powell and Geller, 1999; Kettenmann and Verkhratsky, 2008; Taber and Hurley, 2008; Kriegstein and Alvarez-Buylla, 2009), however, very little is known about the genes necessary for proper astroglial development. Non-biased forward genetic approaches designed to uncover the genes needed for glial development and neural-glia interactions have been largely limited to invertebrate systems, and have uncovered a handful of molecules that are required for nervous system development and function (Chanal and Labouesse, 1997; Klambt et al., 1999). Only one forward genetic screen has focused on vertebrate glial development (zebrafish oligodendrocytes and schwann cells) (Pogoda et al., 2006) and no genetic screens have focused on astroglia.

Over the last two decades a number of zebrafish genetic screens have identified genes necessary for other aspects of vertebrate neural development, including neuronal survival, brain morphogenesis, retinal axon guidance, myelination, as well as CNS functions that drive behavior (Abdelilah et al., 1996; Granato et al., 1996; Jiang et al., 1996; Karlstrom et al., 1996; Odenthal et al., 1996; Schier et al., 1996; Trowe et al., 1996; Gulati-Leekha and Goldman, 2006; Pogoda et al., 2006). The vast majority of these screens employed a chemical mutagen, ethylnitrosourea (ENU), to generate small genetic lesions. While this mutagen is an efficient way to generate large numbers of random mutations, the process of identifying affected loci is often laborious. In contrast, insertional mutagenesis strategies enable the quick identification of disrupted genes by utilizing the inserted DNA sequence as a tag (Gaiano et al., 1996; Amsterdam and Hopkins, 1999). A large-scale retroviral-mediated insertional mutagenesis recently identified approximately 25% of the genes essential for embryonic development (Golling et al., 2002; Amsterdam et al., 2004). Importantly, the genes affected in 325 of the approximately 390 mutated loci have been identified. Several subsequent “shelf screens” using these existing viral insertion lines have identified genes essential for craniofacial development, liver size, cilia and kidney development, eye development, hematopoietic stem cell emergence, and cancer (Sun et al., 2004; Gross et al., 2005; Sadler et al., 2005; Nissen et al., 2006; Burns et al., 2009; Lai et al., 2009).

We present here the results of the first screen of this large insertional mutant collection designed to identify genes affecting axon pathfinding and astroglial development. We screened 274 of 315 previously generated insertional mutant lines (Golling et al., 2002; Amsterdam et al., 2004) using axon and glial specific antibodies. We identified 25 genes required for axon scaffold formation and/or astroglial development. Because the identity of all these genes has already been determined (Amsterdam et al., 2004) this population of mutants provides immediate information on the molecular underpinnings of these phenotypes. These mutants provide a new window into the relationship between axon and glial development in the early CNS.

## Results and Discussion

### Screen overview

The Hopkin's laboratory at MIT generated and identified insertional mutations in 315 genes that lead to visible morphological defects or lethality by five days of development (Golling et al., 2002; Amsterdam and Hopkins, 2004). To screen for axon scaffold and astroglial defects in this mutant collection, we obtained clutches of embryos from identified heterozygote parents, representing insertional mutants for 274 of the 315 identified genes. Embryos were fixed at 40 hours post fertilization (hpf) and labeled using the anti-Acetylated tubulin (AT) and anti-Glial fibrillary acidic protein (Gfap) antibodies (Fig. 1). In a primary screen, we identified 115 mutants with defects in axonal and/or astroglial patterning that segregated by Mendelian ratios (~25% of embryos from each clutch). However, among these 115, 40 also had major cell death (Fig. 2). For example, the *rrm2* insertional mutant exhibited extensive necrosis (data not shown, (Golling et al., 2002)) that was accompanied by dramatic reductions and disorganization in forebrain glia and axons (Fig. 3B). Because axonal and glial defects in these mutants are likely to be secondary effects, we omitted these 40 necrotic mutants from subsequent analysis. Out of the remaining 75 insertional mutants, 24 were eliminated from further analysis based on significant and generally wide spread morphological malformations, most likely due to defects in gastrulation and early germ layer patterning. The remaining mutants had a range of less severe morphological abnormalities that were more tissue/region specific, and these were kept for further analysis. Upon rescreening, 25 of the remaining 51 mutants had phenotypes consistent with those seen in the primary screen. These 25 mutants had different combinations of phenotypes, including defects in the forebrain commissures, optic nerve and chiasm, forebrain astroglia, hindbrain radial glia, hindbrain axons, spinal cord radial glia, and motor axon associated glia. The genes affected in all of these viral insertion lines are known (Table 1).

### Genes affecting forebrain commissure formation

We identified 24 mutants in 21 genes (2 alleles each of *wnt*, *cdh2*, and *pou5f1*) that affected formation of the anterior commissure (AC) in the telencephalon and/or the post optic commissure (POC) in the diencephalon. These 24 mutants had different combinations of defects including reduced commissure size, axon wandering, and/or defasciculation. Mutations in four genes (*mib*, *sfpq*, *smo*, and *utp11l*) led to reduced forebrain commissures (Fig. 3F,J,N), while mutations in five genes (*gnl3*, *pes*, *kif11*, *csnk1a1*, and *chd*) led to axon defasciculation of one or both commissures (Fig. 3D,S,Q,W,X, data not shown). Eight mutants (*mpp5a*, *twistnb*, *ppp1r12a*, *mak16*, *pou5f1*, *abhd11*, *esco2* and *arnt2*) had both reduced and defasciculated commissures (Fig. 3H,K,M,O,P,T,V, data not shown). Four mutations (*wnt5b*<sup>1780B</sup>, *wnt5b*<sup>2735B</sup> *cdh2* and *hnf1b*) led to commissural axon wandering that was paired with defasciculation (Fig. 3C,G,S).

Surprisingly no mutants had commissure defects that were restricted to the AC. Six mutants had defects in both the AC and POC (*wnt5b*<sup>2735B</sup>, *mib*, *twistnb*, *utp11l*, *mak16*, *esco2*), while

16 had POC-specific defects (*wnt5b*<sup>1780B</sup>, *pes*, *pou5f1*, *kif11*, *lamb1*, *chd*, *csnk1a1*, *gnl3*, *cdh2*, *mpp5a*, *sfpq*, *smo*, *ppp1r12a*, *hnf1b*, *abhd11*, and *arnt2*). These findings suggest that formation of the AC utilizes many of the mechanisms that are also responsible for organizing the POC.

The majority of the insertional mutants with forebrain commissure defects affect genes that encode components of signal transduction pathways; either the signals themselves (e.g. *Wnt5b*), enzymatic components of the signal transduction machinery (e.g. *Abhd11*, *Csnk1a1*, *Mib*, *MPP5a*, and *PPP1r12a*), or downstream transcription factors (e.g. *Hnf1b*, *Pes*, *Pou5f1*, and *TwistNB*). As an example, *wnt5b* mutants had a defasciculated POC and commissural axons were seen to grow into inappropriate regions for the forebrain (Fig. 3C). The *wnt5b*<sup>1780b</sup> allele leads to more severe axon defects than the *wnt5b*<sup>2735B</sup> allele, and these are accompanied by more severe morphological phenotypes. Consistently, *wnt5b*<sup>1780b</sup> appears to be a null allele, while *wnt5b*<sup>2735B</sup> may be a hypomorphic allele caused by an intronic insertion that reduces but does not eliminate *wnt5b* transcript (Golling et al., 2002; Amsterdam et al., 2004). The *wnt5b* (*pipetail*) mutant was previously identified based on defects in gastrulation and tail formation (Hammerschmidt et al., 1996), and this mutant has been subsequently used to define the role of *Wnt5b* in embryonic axis formation (Westfall et al., 2003; Marlow et al., 2004). Secreted Wnt proteins are known to influence cell differentiation, but can also act directly to influence cell migration and axon guidance (Freese et al., 2009; Sanchez-Camacho and Bovolenta, 2009). This is similar to the *Hedgehog* (*Hh*) family of signaling proteins (Briscoe, 2009). We previously showed that mutations in *Hh* signaling pathway components lead to POC and optic chiasm defects that likely result from the misregulation of midline guidance cues of the *slit* and *semaphorin* families (see optic nerve mutants below) (Karlstrom et al., 1996; Karlstrom et al., 1999; Barresi et al., 2005). These two *wnt* alleles will provide valuable tools to help determine whether *wnt5b* acts in forebrain patterning and/or directly on commissural axons.

Two commissural mutants had insertions in genes encoding cell adhesion molecules (*lamb1* and *cdh2*). Mutations in *laminin beta 1* (*lamb1*) were associated with all three commissural phenotypes: POC reduction, defasciculation, and axon wandering (Fig. 3R). *Lamb1* is a cell adhesion molecule important for mediating cell/extracellular matrix interactions. Previous zebrafish screens identified mutations in *lamb1* (the *grumpy* mutation) and *laminin alpha 1* (the *bashful* mutant) based on notochord and CNS defects (Brand et al., 1996; Karlstrom et al., 1996; Odenthal et al., 1996; Schier et al., 1996). It was subsequently shown that *lamb1* is critical for basement membrane formation in the notochord and eye (Parsons et al., 2002; Lee and Gross, 2007). *lama1* was also shown to be necessary for proper formation of most axonal tracts in the CNS (Paulus and Halloran, 2006). Our findings, together with these past studies, support an important role for Laminin proteins in the formation the embryonic axonal scaffold of the CNS. Finally, the identification of commissure defects in mutants affecting the homophilic cell adhesion molecule Cadherin 2 (*cdh2*, previously named *parachute* (Jiang et al., 1996; Lele et al., 2002)) (Fig. 3G), suggests *Cdh2* (also known as N-Cadherin) may mediate axon-substrate cell adhesion during commissure formation. Based on our phenotypic analysis (see section below on mutants affecting astroglia in the forebrain) we hypothesize that *cdh2* is required for interactions between commissural axons and forebrain astroglia (Barresi et al., 2005).

### Genes affecting optic nerve and chiasm formation

In all vertebrates, retinal ganglion cells (RGCs) extend axons that exit the eye and grow across the midline of the diencephalon to form the optic nerves and optic chiasm. In zebrafish, all RGC axons cross the midline at the optic chiasm and continue to grow to their targets in the contralateral tectal lobe (Stuermer, 1988). The anti-Acetylated Tubulin antibody labels RGC axons, allowing us to assess formation of the optic nerve and optic

chiasm ((Chitnis and Kuwada, 1990; Wilson et al., 1990) Fig. 1C, arrowheads and arrow respectively). We identified 17 mutations that affected retinal axon projections. These phenotypes were grouped into four categories: optic nerve reduction, optic nerve thickening, optic nerve defasciculation, and RGC axon mistargeting (Table 1).

In 10 mutants, representative of 9 genes, (*gnl3*, *bysl*, *chd*, *hnfb1*, *pou5f1*, *pes*, *lamb1*, *abhd11* and *esco2*) the optic nerves from each eye were reduced in thickness, most likely because fewer RGC axons reached the midline (Fig. 3, data not shown). In contrast, the notch pathway mutant, *mindbomb* (*mib*), led to a dramatic increase in the thickness of the optic nerve (Fig. 3F, arrowheads, bracket). Despite these defects, RGC axons crossed the midline normally in *mib* mutants (Fig. 3F, arrow). *mib* mutants (previously named *whitetail*) were first identified based on defects in neural development (Jiang et al., 1996; Schier et al., 1996). *mib* was subsequently shown to be required for the formation of a variety of embryonic tissues including the hindbrain (Bingham et al., 2003), retina (Bernardos et al., 2005), and ear (Haddon et al., 1998). *mib* encodes a ubiquitin ligase directly required for Delta-Notch signaling, and loss of *mib* function is associated with increased neuronal differentiation (Itoh et al., 2003). The presence of thicker optic nerves in *mib* mutants is consistent with an increase in RGC (and thus RGC axon) numbers. Intriguingly, the POC was reduced in *mib* mutants. This suggests distinct roles for notch signaling in adjacent nerve pathways. As with Wnt signaling, loss of Notch signaling may disrupt cell differentiation of neurons and glia in the POC region and/or may directly disrupt axon guidance mechanisms.

In three of the 17 optic nerve mutants (*cadherin2* (*cdh2*), *mpp5a*, and *copa*), RGC axons appropriately crossed the midline to form the optic chiasm, however the optic nerves were highly defasciculated and were split into several separate individual axon bundles (Fig. 3G,H,I,I' and data not shown). Defasciculation of the optic nerve in *cdh2* (*N-Cadherin*) mutants may be due to a role in homophilic cell adhesion between axons (Masai et al., 2003; Suzuki and Takeichi, 2008) or between axons and glia. The *mpp5a* locus was previously identified and named *nagie oko* based on retinal phenotypes (Malicki et al., 1996). *mpp5a* encodes a membrane associated apical junction protein of the MAGUK family (Wei and Malicki, 2002). *mpp5a* is required for proper lamination within the retina as well as for the apicobasal organization of neuroepithelia in the embryo (Wei et al., 2006 Zolessi, 2006 #1719; Zou et al., 2008; Yang et al., 2009). This suggests defasciculation of the optic nerve in *mpp5a* mutants may be due to retinal lamination defects or to disrupted interactions between pathfinding axons and their cellular substrate. *copa* encodes the  $\alpha$  subunit of the coatamer protein complex, and is responsible for maintenance of Golgi bodies and recycling transport machinery (Coutinho et al., 2004). Since the ability to transport axon guidance receptors to and from the cellular membrane is critical for axon pathfinding (Sann et al., 2009), the *copa* mutant may provide insight into the molecular machinery linking receptor turnover and axon fasciculation.

Finally, four mutations (*smo*<sup>hi229</sup>, *wnt5b*<sup>1780B</sup>, *sfpq*, and *ppp1r12a*) led to RGC pathfinding defects that included ipsilateral RGC axon projections (Fig. 3C,J,L; Sup.Mov.1; data not shown) similar to those seen in Hedgehog pathway mutants (Culverwell and Karlstrom, 2002). In fact, *smo*<sup>hi229</sup> affects the well-characterized Hh receptor-complex gene *smoothened* (Chen et al., 2001; Varga et al., 2001). Axons likely project ipsilaterally in *smo*<sup>hi229</sup> due to defects in the midline growth substrate as shown for the Hh pathway mutants *yot*(*gli2*) and *dtr*(*gli1*) (Barresi et al., 2005). *wnt5b* mutants displayed RGC and POC axon pathfinding errors that were similar to, but less severe than, *smo* mutants (Fig. 3C). *sfpq* mutants had more specific RGC pathfinding errors (Sup.Mov.1), while *ppp1r2a* mutants also had ipsilateral projections that were accompanied by reduced optic nerves. *sfpq* encodes the PSF protein (polypyrimidine tract-binding protein-associated splicing factor)



that was recently shown to be important for selective neuronal survival and proper brain ventricle formation (Lowery et al., 2007; Lowery et al., 2009) suggesting axon defects in these mutants are likely secondary to defects in earlier brain patterning.

### Genes affecting astroglia in the forebrain

In both the zebrafish and mouse, astroglial cells are tightly associated with the forebrain commissures and the optic chiasm (Mason and Sretavan, 1997; Barresi et al., 2005; Lindwall et al., 2007). In zebrafish, forebrain astroglia form two tight “bridges” that span the midline at the position of the AC in the telencephalon and the POC in the diencephalon, with astroglia being largely excluded from the region between the commissures (Fig. 1A, bracket, (Barresi et al., 2005)). We identified 21 mutants in 19 genes (2 alleles each of *wnt5b* and *pou5f1*) with forebrain astroglial phenotypes. Similar to the commissural axon mutants, no mutants had astroglial defects that were confined to the telencephalon. 12 mutants had astroglial defects in both the telencephalon and diencephalon (*gnl3*, *pou5f1*, *mib*, *arnt2*, *sfpq*, *ppp1r12a*, *esco2*, *utp11l*, *mak16*, *wnt5b*<sup>2735B</sup>, *twistnb*, and *kif11*), while 8 mutants had defects that were restricted to the diencephalon (*wnt5b*<sup>1780B</sup>, *pes*, *lamb1*, *csnk1a1*, *mpp5a*, *abhd11*, *smo*, and *chd*) (Table 1, Fig. 3, data not shown). Again, this lack of telencephalon-specific astroglial phenotypes suggests common patterning mechanisms in both parts of the brain.

Forebrain astroglia were reduced and disorganized in four mutants (*mib*, *twistnb*, *utp11l*, and *lamb*), with Gfap<sup>+</sup> cells mis-located between the commissures (Fig. 3F,K,N,R). In 16 mutants (*wnt5b*<sup>1780B/2735B</sup>, *gnl3*, *mpp5a*, *sfpq*, *smo*, *ppp1r12a*, *mak16*, *pou5f1*<sup>349/1940</sup>, *pes*, *abhd11*, *esco2*, *csnk1a1*, *arnt2*, and *chd*) the forebrain astroglial bridges were similarly disorganized but astroglial cell numbers appeared to be normal (Fig. 3, data not shown). Among this group, the *casein kinase 1a1* (*csnk1a1*) mutation led to a unique phenotype, with long fibrous Gfap positive structures located between the commissures (Fig. 3X, inset). Finally, mutations in the kinesin family gene *kif11* led to an increase in the number of Gfap expressing cell bodies in the ventricular regions of the forebrain (Fig. 3W, inset), hindbrain and spinal cord (see hindbrain and spinal cord sections below). Changes in astroglial cell numbers might be caused by misregulation of cellular mechanisms controlling proliferation, differentiation, migration, and/or survival. Defects in astroglial organization are likely due to disrupted forebrain patterning and/or directed cell migration. We have shown previously that diencephalic astroglia respond to changes in Slit guidance cues, suggesting that the mechanisms underlying proper glial positioning in the forebrain may be similar to those that guide commissural and RGC axons (Barresi et al., 2005).

### Astroglia and the formation of the forebrain axon scaffold

The simultaneous detection of both axonal and astroglial defects in this screen has provided new insight into how these two cell types interact in formation of the forebrain axon scaffold. Intriguingly, no mutants were identified in which astroglial defects were independent of closely related axon scaffold defects (Fig. 2). Mis-positioned axons were always precisely associated with and seemed to contact mis-positioned astroglial cells. Since astroglial cells form bands that span the midline in the POC and AC regions prior to axon outgrowth (Barresi et al., 2005), these results are consistent with the idea that astroglia provide guidance cues for commissural and retinal axons as they extend across the forebrain.

Two mutants were identified in which axon defects were uncoupled from glial defects. These mutants may provide insights into the molecular basis of axon-glial interactions. *hmf1b* and *cdh2* mutants had clear forebrain axon scaffold defects but forebrain glia appeared to be patterned normally (Fig. 3G,S). Since Cadherin is a homophilic adhesion molecule (Thiery, 2003; Suzuki and Takeichi, 2008) the *cdh2* phenotype may indicate that Cdh2-

mediated cell-cell adhesion is required for proper axon-glia interactions. Hnf1b is a transcription factor that is known to regulate the expression of a variety of downstream genes including cell adhesion molecules such as E-Cadherin and L-CAM (Goomer et al., 1994; Yamagata et al., 2002). While *hnf1b* has been shown to be important for rhombomere development in the hindbrain (Sun and Hopkins, 2001; Wiertel and Sive, 2003; Choe et al., 2008), we did not detect consistent hindbrain defects in axons or glia in *hnf1b* mutants (see below).

### Genes affecting radial glia in the hindbrain

Similar to the cortex of the mouse brain, the zebrafish hindbrain contains radial glial cell bodies that are positioned ventrally and extend radial processes dorsally to the pial surface where they terminate in endfeet (Fig. 2D, 4A, brackets; (Trevarrow et al., 1990; Gotz, 1995; Kim et al., 2008). We identified 17 viral insertions (2 each for *cdh2* and *pou5f1*) in 15 genes that disrupt the radial glial morphology in the hindbrain, and we grouped these into four phenotypic categories: reduced glia, disrupted but segmentally patterned glia, disrupted glia with no segmental organization, and ectopic glial clusters (Fig. 4, Table 1). Axon defects always accompanied these glial defects, with mis-positioned axons being tightly associated with mis-positioned glia.

One mutant, *esco2*, had no Gfap labeled structures in the hindbrain (Fig. 4B). This phenotype is similar to that seen in mutants with general cell death, such as *rrm2* (Golling et al., 2002) and may reflect non-specific cell death. Interestingly, *Esco2* (Establishment of Cohesion 1 homolog 2) is required for sister chromatid cohesion following DNA replication, and defects in this gene underlie Roberts Syndrome in humans (Vega et al., 2005; Gordillo et al., 2008; van der Lelij et al., 2009). Roberts Syndrome causes symptoms that include symmetrical limb reductions, craniofacial malformations, and mental retardation (Goh et al.). The zebrafish *esco2* mutant may provide a new model for the study of CNS defects associated with Roberts Syndrome.

Six mutants (*lamb1*, *foxi*, *ppp1r12a*, *mak16*, *smo*, and *pou5f1*) had disorganized radial glial processes that respected normal anterior-posterior segmental borders in the hindbrain. Among these, *lamb1*, *foxi*, and *smo* mutants had normal looking radial glial processes that were abnormally spread within each hindbrain segment (Fig. 4C,D, data not shown). Hindbrain organization, including axon projections, was previously shown to be disorganized in *lamb1a* (*grumpy*) mutants (Schier et al., 1996), suggesting these glial defects may be secondary to more general hindbrain patterning defects. Glial morphology was more severely disrupted in *ppp1r12a*, *mak16*, and *pou5f1* mutants (Fig. 4E-G). Similarly, five mutants (*utp11l*, *arnt2*, *gnl3*, *bysl*, and *wnt5b<sup>1780B</sup>*) also had highly disorganized Gfap labeling throughout the hindbrain, however this phenotype was coupled with disrupted anterior/posterior segmental patterning (Fig. 4H-L).

Finally, three mutants (*mib*, *twistnb*, and *cdh2*) contained clusters of Gfap labeled cells without any recognizable radial glial morphology (Fig. 4M-O). In *mindbomb* (*mib*) mutants, Gfap positive cell clusters were randomly distributed. In contrast, in *twistnb* mutants these glial clusters were concentrated ventrally and Gfap labeled processes were present that spanned the ventral/dorsal axis, similar to the wild type radial process architecture (Fig. 4N). *cadherin2* (*cdh2*) mutants had abnormal clusters of Gfap expressing cells that were restricted to the dorsal hindbrain (Fig. 4M, arrowheads). While hindbrain patterning has been previously shown to be disrupted in *mib* and *cdh2* mutants (Jiang et al., 1996; Bingham et al., 2003), the presence of ectopic glial clusters has not been described.

### Genes affecting the hindbrain axon scaffold

Mutations in nine genes that disrupted hindbrain glia also affected the axon scaffold in the hindbrain. In two mutants, *twistnb* and *mib*, hindbrain axon projections were generally reduced and the remaining axons were closely associated with abnormally clustered and reduced glia (Fig. 4N,O). *cdh2* mutants, like *twistnb* and *mib*, had ectopic glial clusters, but these mutants had expanded (rather than reduced) dorsoventrally projecting axons (Fig. 4M). Hindbrain axon defects were previously shown in *mib* mutants and are likely to be the consequence of earlier hindbrain patterning defects (Bingham et al., 2003). *cdh2* mutants were also previously shown to have disrupted axon projections (Jiang et al., 1996) and ectopic neurons in the dorsal hindbrain (Lele et al., 2002); and we show that these dorsally mis-positioned neurons (Fig. 4M' inset) are directly associated with ectopic glial clusters (Fig. 4M', circles). Since radial glial cells serve as a neural stem cell population (Kriegstein and Alvarez-Buylla, 2009), it would be interesting to determine whether these ectopic astroglial clusters are responsible for generating the ectopic neurons. The fact that these three mutants (*twistnb*, *mib*, and *cdh2*) have mis-positioned axons that are associated with mis-positioned glia lends further support to the hypothesis that astroglia provide a preferred substrate for axon growth.

In three mutants, *ppp1r12a*, *mak16* and *utp11l*, axons were expanded along the dorsoventral axis of the hindbrain. These mis-positioned axons were associated with mis-patterned Gfap expressing cells (Fig. 4E,F,H). Finally, three mutants (*pou5f1*, *arnt2* and *wnt5b<sup>1780B</sup>*) had generally disorganized axons that were located in their normal ventral position in the hindbrain (Fig. 4G,I,L). For technical reasons, AT labeling in the remaining six astroglial mutants (*bysl*, *foxi1*, *gnl3*, *lamb1*, *smo*, and *esco2*) was too faint to resolve axon defects in the hindbrain. Whether these mutants have corresponding axon scaffold defects associated with their astroglial phenotypes remains to be determined.

### Genes affecting radial glia in the spinal cord

An important and unexpected outcome of this screen was the identification of 13 mutants in 12 genes (2 alleles of *pou5f1*) with specific changes in radial glia cell number and/or morphology in the spinal cord (Fig. 5). Radial glial cell bodies in the spinal cord are normally positioned toward the midline, near the ventricle (central canal). These glial cells extend processes radially that terminate with end feet at the pial surface (Kim et al., 2008) (Fig. 1D,5A). This class of mutants had a range of phenotypes, from a complete loss of radial glial cells to increases in the number of Gfap labeled cell bodies. Defects were also seen in radial glial processes. The genes in this class of mutants encode a variety of signaling molecules, phosphatases, transcription factors, and metabolic proteins.

Eight mutants in this class had decreased numbers of glial cells in the ventricular zone of the spinal cord. Ventricular glia were reduced in two of these mutants (*ppp1r12a* and *pou5f1*) (Fig. 5C,D), and completely absent in six mutants (*gnl3*, *twistnb*, *utp11l*, *mak16*, *mib*, and *smo*) (Fig. 5E-H, M,O). In all of these mutants Gfap labeling in the floorplate and roofplate was normal, making them distinct from the non-specific *rrm2* mutant (Fig. 5B) (Golling et al., 2002). Changes in cell-cycle regulation may account for the reduced glia seen in many of these mutants. For example, *mak16* is required for proper rRNA biogenesis in yeast and its loss causes cell cycle arrest in G1 (Wickner, 1988; Pellett and Tracy, 2006). *smo* and *mib* affect Hh and Notch-Delta signaling, respectively, and both pathways have been shown to regulate cell proliferation as well as cell differentiation (Varga et al., 2001; Itoh et al., 2003). The phosphatase *Ppp1r12a* and transcription factors *Pou5f1* (*oct4*) and *Twistnb* are components of signal transduction systems (Kosan and Kunz, 2002; Ito et al., 2004; Lunde et al., 2004), and our data suggest these pathways affect the regulation of radial glial cell



cycle or cell number. An alternative possibility is that misregulation of cell fate decisions in early precursor populations leads to reductions in astroglial cell types.

Three of the 13 mutants in this class of spinal cord radial glial mutants had defects in the pattern of radial glial processes in the spinal cord. *mib* mutations led to a loss of radial glial processes that accompanied the loss of cell bodies described above (Fig. 5M). Surprisingly, Gfap expressing glial processes in the roof plate and floor plate were unaffected in *mib* mutants (Fig. 5M, brackets). Changes in Notch-Delta signaling cause alterations in the differentiation of neurons versus glia in the spinal cord (Park and Appel, 2003; Shin et al., 2007; Kim et al., 2008), suggesting the loss of glial cell bodies and radial processes in *mib* mutants may be due to a shift in cell fates from glia to neurons. In contrast to this loss of radial processes, *ppp1r12a* mutants had ectopic glial processes emanating from unique cell clusters that were located in the dorsal third of the spinal cord (Fig. 5N, arrows). Interestingly, these clusters surrounded ectopic neurons with axonal projections that extended ventrally (Fig. 5N). Lastly, *smo* mutants had disorganized radial processes throughout the spinal cord, despite a general loss of Gfap+ cell bodies in the ventricular zone (5O). Again, these defects in radial glial processes are likely due to earlier requirements for hedgehog signaling in spinal cord development (Briscoe, 2009).

Perhaps most interesting in this class were four mutants (*kif11*, *esco2*, *wnt5b<sup>2735B</sup>*, and *arnt2*) that had increased numbers of well-labeled glial cell bodies in the spinal cord (Fig. 5J-L). The number of Gfap labeled cell bodies was moderately increased in the ventricular zone of *wnt5b<sup>2735B</sup>* mutants (Fig. 5J), while *kif11* and *esco2* mutants had more dramatic increases in the same region (Fig. 5K, L). Specifically, *kif11* mutants had a 4-fold increase in the number of Gfap labeled somas in the spinal cord (MJFB, unpublished data). Interestingly, these same mutants also had enlarged Gfap-labeled cell bodies in the floorplate region. The Gfap labeled cells in the floorplate of *kif11* mutants were 4-times larger in diameter than the glial cell bodies found in the ventricular zone (MJFB, unpublished data). *kif11* and *esco2* mutants had the most of these large floorplate glial cell bodies, while *wnt5b<sup>2735B</sup>* mutants were more variable and had fewer of these cells. Finally, *arnt2* mutants also had Gfap labeled cell bodies in the floorplate, but did not have increased glial cell bodies present in the ventricular zone (Fig. 5I, arrowhead). How this class of mutations impacts the number of Gfap labeled cell bodies at the ventricular zone may be related to the cellular behavior that radial glia exhibit during the process of cell division. Prior to mitosis radial glial cells maintain their characteristic extended morphology, however as cells enter mitosis and begin to divide, somas and cytoplasmic components such as Gfap move to the ventricular zone (Alexandre et al.). Therefore, changes in the number of Gfap labeled cell bodies at the ventricular zone may indicate a change in the percentage of glial cells at a particular stage (e.g M-phase) of the cell cycle.

*kif11* encodes Kinesin family member 11, also known as EG5, a plus-end directed kinesin motor protein that functions in spindle pole separation during mitosis (Sawin et al., 1992; Sawin and Mitchison, 1995; Valentine et al., 2006a; Valentine et al., 2006b). *In vitro* studies show that pharmacological inhibition of EG5 causes mitotic arrest (Miyamoto et al., 2004; Sarli et al., 2005). This role for Kif11 in mitosis has recently made it the focus of new chemotherapies (Mayer et al., 1999; Kapoor et al., 2000; Maliga et al., 2002; DeBonis et al., 2003; Brier et al., 2004; Cochran et al., 2005; Maliga and Mitchison, 2006; Sarli and Giannis, 2006; Klein et al., 2007). Since the somas of radial glia are located at the ventricular zone during M phase of mitosis (Alexandre et al.), we hypothesize that radial glia are arrested or slowed in mitosis in *kif11* mutants, and thus a greater number of cells are detectable in the ventricular zone by Gfap labeling. As new radial glia are produced and attempt to divide they may be trapped in M-Phase, resulting in an increase in Gfap labeled cell bodies in the ventricular zone overtime. Like *kif11* mutants, *esco2* mutants may also be

due to a failure to progress through mitosis. Consistent with this idea, *Esco2* (Establishment of Cohesion 1 homolog 2) is required for sister chromatid cohesion following DNA replication (Vega et al., 2005). Moreover, the increase in glial cells seen in *wnt5b*<sup>2735B</sup> mutants may indicate a role for Wnt signaling proteins in regulating glial cell cycle and proliferation (Freese et al., 2009). Lastly, the protein encoded by the *arnt2* locus, *aryl hydrocarbon receptor nuclear translocator 2*, binds directly to the Aryl hydrocarbon receptor (AhR) and acts as a transcriptional cofactor to regulate gene expression affiliated with Dioxin toxicity responses (Beischlag et al., 2008; Perdew, 2008). *arnt2* mutations have been implicated in tumorigenesis and may thus play a role in cell proliferation (Carney et al., 2006). Consistently, the AhR is suggested to cause cell cycle arrest in liver cells through association with the Retinoblastoma tumor suppressor (Huang and Elferink, 2005). The fact that we observe increased numbers of Gfap labeled cell bodies only in the floorplate of *arnt2* mutants suggests *Arnt2* may affect cell cycle progression in a more cell-type or region specific manner than *Kif11*, *Esco2* and *Wnt5b*.

These mutants that affect astroglial cell number represent a particularly important class of genes, because radial glial cells are the primary neural stem cell population in vertebrate embryos and neonates (Kriegstein and Alvarez-Buylla, 2009; Lam et al., 2009) and misregulation of cell cycle may lead to most if not all congenital brain tumors (Wechsler-Reya R, 2001; Ruiz i Altaba et al., 2004; Jackson and Alvarez-Buylla, 2008). In fact a recent study showed that a congenital subependymal giant cell astrocytoma expressed many of the known neural stem cell and radial glial markers, providing strong evidence that this tumor may be derived from misregulated radial glial cells (Phi et al., 2008). Understanding this new class of mutants is likely to provide insight into the cell-cycle regulation of neural stem cells that could potentially lead to better cancer therapies.

### Genes affecting motor nerves in the trunk

We identified 11 mutations in 10 genes (2 alleles of *cdh2*) that disrupt Gfap labeling of motor nerves in the trunk (Fig. 2E, 6A). Because of the demonstrated specificity of the anti-Goldfish Gfap antibody (Nona et al., 1989; Marcus and Easter, 1995), we hypothesize that this antibody labels a population of glia (Fig. 6A'') that are tightly associated with anti-Acetylated Tubulin labeled motor axons (Fig. 6A'). Currently two types of glia have been shown to wrap motor axons in zebrafish. Schwann cells begin to wrap motor axons at 24 hpf, while perineurial glia wrap axons starting at about 45 hpf (Kucenas et al., 2008). Since our screen was performed on 40 hpf embryos, the cells examined in this study are most likely Schwann cells. Because the tools to test this hypothesis are not currently available, we will describe the phenotypes in anti-Gfap labeling as affecting *motor axon-associated glia*.

Four mutants (*sfpq*, *ppp1r12a*, *twistnb*, and *mak16*) had reduced motor axons and associated glia in the trunk. *sfpq* mutants had a near complete loss of motor axon-associated glia (Fig. 6C, arrows). In *ppp1r12a* mutants motor nerves were truncated, terminating dorsal to the horizontal myoseptum (Fig. 6B). *twistnb* mutants had varying degrees of motor axon-associated glial truncations, ranging from a complete loss in some segments to shortened nerves in other segments (Fig. 6D). Finally, *mak16* mutants had truncated motor axon associated glia, but in only a few segments of each labeled embryo (Fig. 6E, arrowhead). It is unknown whether the presence of motor axons influences the timing, organization and positioning of these associated glial cells. These four mutants may help shed light on the relationship between axons and glia in the formation of motor nerves.

Two mutants (*wnt5b*<sup>1780B</sup> and *copa*) had excessively branched motor axon-associated glia (Fig. 6F,G, arrowheads). *wnt5b*<sup>1780B</sup> mutants also had variable motor nerve truncations, while in *copa* mutants motor axon-associated glia were present in the appropriate ventral location in most segments. Interestingly, some motor axons still navigated correctly to their

ventral location in *wnt5b*<sup>1780B</sup> mutants despite aberrant branching and truncation of associated glia (Fig. 6F, inset). It has been shown that Wnt5b, along with two other Wnts, is an important signal for motorneuron cell fate in the mouse spinal cord (Agalliu et al., 2009). Based on our findings it would be interesting to see if Schwann cells or other associated glia are similarly disrupted in the *wnt5b* knock-out mouse.

*cadherin2* (*cdh2*), *esco2*, *tbx16*, and *smo* mutants had distinct trunk defects that did not fit into the categories described above. In *cdh2* mutants, Gfap labeled processes were dramatically disorganized. These labeled glial processes were kinked, had multiple connections to the spinal cord, and were variably truncated (Fig. 6H); phenotypes that are consistent with a loss of cell-cell adhesion. Importantly, *cadherin2* is expressed by both motorneurons and glia, and has been shown to be necessary in Schwann cells to induce motorneuron outgrowth in vitro (Bixby et al., 1988; Tomaselli et al., 1988; Bixby and Zhang, 1990; Marthiens et al., 2002). The *cdh2* zebrafish mutants may provide a unique model to study Cadherin mediated axon-glial interactions during motor nerve development.

*esco2* mutants had punctate Gfap labeling in the spinal cord that also extended along motor axons in the trunk (Fig. 6I). *tbx16* (formerly called *spadetail* (Ho and Kane, 1990)) mutants had ectopic Gfap labeling at the ventral ends of presumptive motor axons (Fig. 6J, arrowheads). In some somites the ectopic glia formed connections across adjacent segments (Fig. 6J, bracket). *tbx16* is known to affect somite development and axon pathfinding in some regions of the trunk (Ho and Kane, 1990; Tokumoto et al., 1995), and glial defects may also be regionally restricted. Lastly, we confirmed that *smo* mutants have severe reductions in the motor axons (Fig. 6K; data not shown) that are due to the loss of Hh-mediated motorneuron differentiation (Schauerte et al., 1998; Chen et al., 2001; Varga et al., 2001). Intriguingly, we observed ectopic clusters of glia at the location where motor axons would typically exit the neural tube (Fig. 6K, brackets). These glial clusters extended long processes in some segments (Fig. 6K, arrows). In rare cases motor neurons exited the spinal cord but glia were not localized adjacent to the motor nerve (Fig. 6K, inset, arrowheads, green), suggesting *smo* mediated Hh signaling may also affect the ability of glial cells to associate with motor axons.

### Summary: A diverse set of 25 genes essential for nervous system development

The insertional mutagenesis that formed the basis of our glial/axonal screen established a pool of over 300 identified mutants that cause morphological defects or lethality by day 5 of zebrafish development (Amsterdam et al., 2004). The loci identified in this screen encode proteins required for a variety of embryonic and cellular processes including developmental signaling, cell proliferation, transcriptional regulation, and general cellular physiology. Given this pool of mutant lines, it is not surprising that a large number of the astroglial/axonal phenotypes we identified were broad in scope and may be the result of more general embryonic or cellular defects. However, given the pleiotropic roles for most developmentally important genes, these more general mutants nonetheless promise to reveal important regulators of neural and or glial development. An example is the previously identified *mindbomb* (*mib*) mutant, which affects Notch signaling. While *mib* previously implicated Notch signaling in the development of the somites, ear, pancreas, intestine, kidney, and in the processes of hematopoiesis, lymphopoiesis, and neuronal differentiation (Haddon et al., 1998; Itoh et al., 2003; Barsi et al., 2005; Crosnier et al., 2005; Koo et al., 2005; Yoo et al., 2006; Akanuma et al., 2007; Choe et al., 2007; Koo et al., 2007; Liu et al., 2007; Dutta et al., 2008; Hegde et al., 2008; Song et al., 2008; Jeong et al., 2009; Yeo, 2009), our screen uncovered new roles for notch signaling in forebrain axon scaffold formation and astroglial development throughout the CNS.

This screen identified 25 essential genes for neuronal and glial development and all of the mutant loci have been identified. Approximately half of these mutations are in genes not previously linked to development of the embryonic nervous system, and thus they promise to provide insight into new mechanisms regulating CNS development. The remainder of the identified genes have been more extensively studied, but have not been implicated in axon guidance and glial patterning. Over 30% of the identified mutants stand out as having subtle and/or regionally specific defects in neuronal and glial development. The identification of these more specific phenotypes underscores the importance of this mutant collection as a resource for subsequent “shelf screens”. These 25 genes function in a wide spectrum of cellular and developmental processes including germ layer organization, cell cycle progression and cell proliferation, cell-cell signaling and transcriptional regulation, neuronal migration and axon guidance, and cellular physiology. This diversity of gene function underscores the complexity of nervous system development, and these identified mutants will surely provide a valuable resource to stretch our understanding of the genetic, molecular and cellular mechanisms governing how the CNS is built.

## Experimental Procedures

The fish lines used were insertional mutants whose creation was previously described (Amsterdam and Hopkins, 2004). Mutant zebrafish lines were maintained in both two hybrid Tubingen/AB (TAB-5 and TAB-14) backgrounds at the MIT zebrafish facility. Currently, these fish lines can be obtained from the Zebrafish International Resource Center (ZIRC). Embryos were raised at 28.5°C in embryo medium containing 0.003% 1-phenyl-2-thiourea (PTU) to reduce pigmentation (Westerfield, 2007). Embryos were grown to 40 hours post fertilization (hpf) and fixed for immunohistochemistry in 4% formaldehyde (Ted Pella). Antibody labeling was performed as previously described (Barresi et al., 2005) with the exception that Proteinase K treatment was performed for 22 minutes. All antibodies were diluted in blocking solution [PBS, 0.1% Triton-X-100, 2% BSA, 5% NGS, 1% DMSO] and applied overnight at 4°C. Primary antibodies were a rabbit anti-goldfish Glial fibrillary acidic protein (Gfap) polyclonal antibody (Nona et al., 1989; Marcus and Easter, 1995) (1:400 dilution) and a mouse anti-Acetylated Tubulin (AT) monoclonal antibody (1:800 dilution) (Wilson et al., 1990). Fluorescent secondary antibodies (Jackson Immunolabs) were goat anti-rabbit conjugated to Texas Red (1:500 dilution) and goat anti-mouse conjugated to Cy2 (1:200 dilution).

After labeling, embryos were cleared in 75% Glycerol. After removing the yolk, the forebrain was severed from the brain for frontal/ventral mounting, while the remaining hindbrain and trunk were mounted laterally. Epifluorescent imaging was performed using a Zeiss Axioplan2 or Axio-imager. When the Axio-imager was used structural illumination with an Apotome was conducted. For structural illumination, Z-stacks were captured using slices of 0.53µm optimal thicknesses with a number of slices ranging from 48 to 106. XY maximum intensity projections were generated using Axiovision software. All of the images presented in this paper are maximum intensity projections from structural illuminated Z-stacks with the exception of Figs. 3I,J,U, 4C,D, 5N, and 6J which are single epifluorescent images. Forebrain images are frontal/ventral views, presented with anterior up. Images of the hindbrain and trunk are lateral views, dorsal up and anterior to the left.

## Supplementary Material

Refer to Web version on PubMed Central for supplementary material.

## Acknowledgments

We thank Sarah Farrington and Eric Swindell for assisting in collecting and providing fixed embryos for this analysis. We thank Dr. Samuel Nona for providing us with the Anti-Goldfish Gfap antibody. We additionally thank Sarah Farrington, Kate Anderson, and Meg Cunningham for maintenance of fish lines, and Tim Angelini and Chris Doller for general fish husbandry. Lastly, we thank Dr. Stephen Devoto for his helpful comments on this manuscript. This work was supported by NIH grants T32MH020051 and F32NS043872 and NSF grant IOS-0615594 awarded to MJFB and NIH RO1NS039994 to ROK.

## References

- Abdelilah S, Mountcastle-Shah E, Harvey M, Solnica-Krezel L, Schier AF, Stemple DL, Malicki J, Neuhauss SC, Zwartkruis F, Stainier DY, Rangini Z, Driever W. Mutations affecting neural survival in the zebrafish *Danio rerio*. *Development*. 1996; 123:217–227. [PubMed: 9007242]
- Agalliu D, Takada S, Agalliu I, McMahon AP, Jessell TM. Motor neurons with axial muscle projections specified by Wnt4/5 signaling. *Neuron*. 2009; 61:708–720. [PubMed: 19285468]
- Akanuma T, Koshida S, Kawamura A, Kishimoto Y, Takada S. Paf1 complex homologues are required for Notch-regulated transcription during somite segmentation. *EMBO Rep*. 2007; 8:858–863. [PubMed: 17721442]
- Alexandre P, Reugels AM, Barker D, Blanc E, Clarke JD. Neurons derive from the more apical daughter in asymmetric divisions in the zebrafish neural tube. *Nat Neurosci*. 2010; 13:673–679. [PubMed: 20453852]
- Amsterdam A, Hopkins N. Retrovirus-mediated insertional mutagenesis in zebrafish. *Methods Cell Biol*. 1999; 60:87–98. [PubMed: 9891332]
- Amsterdam A, Hopkins N. Retroviral-mediated insertional mutagenesis in zebrafish. *Methods Cell Biol*. 2004; 77:3–20. [PubMed: 15602903]
- Amsterdam A, Nissen RM, Sun Z, Swindell EC, Farrington S, Hopkins N. Identification of 315 genes essential for early zebrafish development. *Proc Natl Acad Sci U S A*. 2004; 101:12792–12797. [PubMed: 15256591]
- Barresi MJ, Hutson LD, Chien CB, Karlstrom RO. Hedgehog regulated Slit expression determines commissure and glial cell position in the zebrafish forebrain. *Development*. 2005; 132:3643–3656. [PubMed: 16033800]
- Barsi JC, Rajendra R, Wu JI, Artzt K. Mind bomb1 is a ubiquitin ligase essential for mouse embryonic development and Notch signaling. *Mech Dev*. 2005; 122:1106–1117. [PubMed: 16061358]
- Beischlag TV, Luis Morales J, Hollingshead BD, Perdew GH. The aryl hydrocarbon receptor complex and the control of gene expression. *Crit Rev Eukaryot Gene Expr*. 2008; 18:207–250. [PubMed: 18540824]
- Bernardos RL, Barthel LK, Meyers JR, Raymond PA. Late-stage neuronal progenitors in the retina are radial Muller glia that function as retinal stem cells. *J Neurosci*. 2007; 27:7028–7040. [PubMed: 17596452]
- Bernardos RL, Lentz SI, Wolfe MS, Raymond PA. Notch-Delta signaling is required for spatial patterning and Muller glia differentiation in the zebrafish retina. *Dev Biol*. 2005; 278:381–395. [PubMed: 15680358]
- Bingham S, Chaudhari S, Vanderlaan G, Itoh M, Chitnis A, Chandrasekhar A. Neurogenic phenotype of mind bomb mutants leads to severe patterning defects in the zebrafish hindbrain. *Dev Dyn*. 2003; 228:451–463. [PubMed: 14579383]
- Bixby JL, Lilien J, Reichardt LF. Identification of the major proteins that promote neuronal process outgrowth on Schwann cells in vitro. *J Cell Biol*. 1988; 107:353–361. [PubMed: 3392103]
- Bixby JL, Zhang R. Purified N-cadherin is a potent substrate for the rapid induction of neurite outgrowth. *J Cell Biol*. 1990; 110:1253–1260. [PubMed: 2324197]
- Brand M, Heisenberg CP, Warga RM, Pelegri F, Karlstrom RO, Beuchle D, Picker A, Jiang YJ, Furutani-Seiki M, van Eeden FJ, Granato M, Haffter P, Hammerschmidt M, Kane DA, Kelsh RN, Mullins MC, Odenthal J, Nusslein-Volhard C. Mutations affecting development of the midline and general body shape during zebrafish embryogenesis. *Development*. 1996; 123:129–142. [PubMed: 9007235]



- Brier S, Lemaire D, Debonis S, Forest E, Kozielski F. Identification of the protein binding region of S-trityl-L-cysteine, a new potent inhibitor of the mitotic kinesin Eg5. *Biochemistry*. 2004; 43:13072–13082. [PubMed: 15476401]
- Briscoe J. Making a grade: Sonic Hedgehog signalling and the control of neural cell fate. *EMBO J*. 2009; 28:457–465. [PubMed: 19197245]
- Burns CE, Galloway JL, Smith AC, Keefe MD, Cashman TJ, Paik EJ, Mayhall EA, Amsterdam AH, Zon LI. A genetic screen in zebrafish defines a hierarchical network of pathways required for hematopoietic stem cell emergence. *Blood*. 2009; 113:5776–5782. [PubMed: 19332767]
- Campbell K, Gotz M. Radial glia: multi-purpose cells for vertebrate brain development. *Trends Neurosci*. 2002; 25:235–238. [PubMed: 11972958]
- Carney SA, Prasch AL, Heideman W, Peterson RE. Understanding dioxin developmental toxicity using the zebrafish model. *Birth Defects Res A Clin Mol Teratol*. 2006; 76:7–18. [PubMed: 16333842]
- Chanal P, Labouesse M. A screen for genetic loci required for hypodermal cell and glial-like cell development during *Caenorhabditis elegans* embryogenesis. *Genetics*. 1997; 146:207–226. [PubMed: 9136011]
- Chanas-Sacre G, Rogister B, Moonen G, Leprince P. Radial glia phenotype: origin, regulation, and transdifferentiation. *J Neurosci Res*. 2000; 61:357–363. [PubMed: 10931521]
- Chen W, Burgess S, Hopkins N. Analysis of the zebrafish smoothed mutant reveals conserved and divergent functions of hedgehog activity. *Development*. 2001; 128:2385–2396. [PubMed: 11493557]
- Chitnis AB, Kuwada JY. Axonogenesis in the brain of zebrafish embryos. *J Neurosci*. 1990; 10:1892–1905. [PubMed: 2355256]
- Choe EA, Liao L, Zhou JY, Cheng D, Duong DM, Jin P, Tsai LH, Peng J. Neuronal morphogenesis is regulated by the interplay between cyclin-dependent kinase 5 and the ubiquitin ligase mind bomb 1. *J Neurosci*. 2007; 27:9503–9512. [PubMed: 17728463]
- Choe SK, Hirsch N, Zhang X, Sagerstrom CG. *hnf1b* genes in zebrafish hindbrain development. *Zebrafish*. 2008; 5:179–187. [PubMed: 18945197]
- Cochran JC, Gatial JE 3rd, Kapoor TM, Gilbert SP. Monastrol inhibition of the mitotic kinesin Eg5. *J Biol Chem*. 2005; 280:12658–12667. [PubMed: 15665380]
- Coutinho P, Parsons MJ, Thomas KA, Hirst EM, Saude L, Campos I, Williams PH, Stemple DL. Differential requirements for COPI transport during vertebrate early development. *Dev Cell*. 2004; 7:547–558. [PubMed: 15469843]
- Crosnier C, Vargesson N, Gschmeissner S, Ariza-McNaughton L, Morrison A, Lewis J. Delta-Notch signalling controls commitment to a secretory fate in the zebrafish intestine. *Development*. 2005; 132:1093–1104. [PubMed: 15689380]
- Culverwell J, Karlstrom RO. Making the connection: retinal axon guidance in the zebrafish. *Semin Cell Dev Biol*. 2002; 13:497–506. [PubMed: 12468253]
- DeBonis S, Simorre JP, Crevel I, Lebeau L, Skoufias DA, Blangy A, Ebel C, Gans P, Cross R, Hackney DD, Wade RH, Kozielski F. Interaction of the mitotic inhibitor monastrol with human kinesin Eg5. *Biochemistry*. 2003; 42:338–349. [PubMed: 12525161]
- Dutta S, Dietrich JE, Westerfield M, Varga ZM. Notch signaling regulates endocrine cell specification in the zebrafish anterior pituitary. *Dev Biol*. 2008; 319:248–257. [PubMed: 18534570]
- Freese JL, Pino D, Pleasure SJ. Wnt signaling in development and disease. *Neurobiol Dis*. 2009
- Gaiano N, Amsterdam A, Kawakami K, Allende M, Becker T, Hopkins N. Insertional mutagenesis and rapid cloning of essential genes in zebrafish. *Nature*. 1996; 383:829–832. [PubMed: 8893009]
- Goh ES, Li C, Horsburgh S, Kasai Y, Kolomietz E, Morel CF. The Roberts syndrome/SC phocomelia spectrum--a case report of an adult with review of the literature. *Am J Med Genet A*. 152A:472–478. [PubMed: 20101700]
- Golling G, Amsterdam A, Sun Z, Antonelli M, Maldonado E, Chen W, Burgess S, Haldi M, Artzt K, Farrington S, Lin SY, Nissen RM, Hopkins N. Insertional mutagenesis in zebrafish rapidly identifies genes essential for early vertebrate development. *Nat Genet*. 2002; 31:135–140. [PubMed: 12006978]

- Goomer RS, Holst BD, Wood IC, Jones FS, Edelman GM. Regulation in vitro of an L-CAM enhancer by homeobox genes HoxD9 and HNF-1. *Proc Natl Acad Sci U S A*. 1994; 91:7985–7989. [PubMed: 7914699]
- Gordillo M, Vega H, Trainer AH, Hou F, Sakai N, Luque R, Kayserili H, Basaran S, Skovby F, Hennekam RC, Uzielli ML, Schnur RE, Manouvrier S, Chang S, Blair E, Hurst JA, Forzano F, Meins M, Simola KO, Raas-Rothschild A, Schultz RA, McDaniel LD, Ozono K, Inui K, Zou H, Jabs EW. The molecular mechanism underlying Roberts syndrome involves loss of ESCO2 acetyltransferase activity. *Hum Mol Genet*. 2008; 17:2172–2180. [PubMed: 18411254]
- Gotz M. Getting there and being there in the cerebral cortex. *Experientia*. 1995; 51:301–316. [PubMed: 7729495]
- Granato M, van Eeden FJ, Schach U, Trowe T, Brand M, Furutani-Seiki M, Haffter P, Hammerschmidt M, Heisenberg CP, Jiang YJ, Kane DA, Kelsh RN, Mullins MC, Odenthal J, Nusslein-Volhard C. Genes controlling and mediating locomotion behavior of the zebrafish embryo and larva. *Development*. 1996; 123:399–413. [PubMed: 9007258]
- Gross JM, Perkins BD, Amsterdam A, Egana A, Darland T, Matsui JI, Sciascia S, Hopkins N, Dowling JE. Identification of zebrafish insertional mutants with defects in visual system development and function. *Genetics*. 2005; 170:245–261. [PubMed: 15716491]
- Gulati-Leekha A, Goldman D. A reporter-assisted mutagenesis screen using alpha 1-tubulin-GFP transgenic zebrafish uncovers missteps during neuronal development and axonogenesis. *Dev Biol*. 2006; 296:29–47. [PubMed: 16784739]
- Haddon C, Jiang YJ, Smithers L, Lewis J. Delta-Notch signalling and the patterning of sensory cell differentiation in the zebrafish ear: evidence from the mind bomb mutant. *Development*. 1998; 125:4637–4644. [PubMed: 9806913]
- Hammerschmidt M, Pelegri F, Mullins MC, Kane DA, Brand M, van Eeden FJ, Furutani-Seiki M, Granato M, Haffter P, Heisenberg CP, Jiang YJ, Kelsh RN, Odenthal J, Warga RM, Nusslein-Volhard C. Mutations affecting morphogenesis during gastrulation and tail formation in the zebrafish, *Danio rerio*. *Development*. 1996; 123:143–151. [PubMed: 9007236]
- Hegde A, Qiu NC, Qiu X, Ho SH, Tay KQ, George J, Ng FS, Govindarajan KR, Gong Z, Mathavan S, Jiang YJ. Genomewide expression analysis in zebrafish mind bomb alleles with pancreas defects of different severity identifies putative Notch responsive genes. *PLoS One*. 2008; 3:e1479. [PubMed: 18213387]
- Ho RK, Kane DA. Cell-autonomous action of zebrafish spt-1 mutation in specific mesodermal precursors. *Nature*. 1990; 348:728–730. [PubMed: 2259382]
- Huang G, Elferink CJ. Multiple mechanisms are involved in Ah receptor-mediated cell cycle arrest. *Mol Pharmacol*. 2005; 67:88–96. [PubMed: 15492120]
- Ito M, Nakano T, Erdodi F, Hartshorne DJ. Myosin phosphatase: structure, regulation and function. *Mol Cell Biochem*. 2004; 259:197–209. [PubMed: 15124925]
- Itoh M, Kim CH, Palardy G, Oda T, Jiang YJ, Maust D, Yeo SY, Lorick K, Wright GJ, Ariza-McNaughton L, Weissman AM, Lewis J, Chandrasekharappa SC, Chitnis AB. Mind bomb is a ubiquitin ligase that is essential for efficient activation of Notch signaling by Delta. *Dev Cell*. 2003; 4:67–82. [PubMed: 12530964]
- Jackson EL, Alvarez-Buylla A. Characterization of Adult Neural Stem Cells and Their Relation to Brain Tumors. *Cells Tissues Organs*. 2008
- Jeong HW, Jeon US, Koo BK, Kim WY, Im SK, Shin J, Cho Y, Kim J, Kong YY. Inactivation of Notch signaling in the renal collecting duct causes nephrogenic diabetes insipidus in mice. *J Clin Invest*. 2009; 119:3290–3300. [PubMed: 19855135]
- Jiang YJ, Brand M, Heisenberg CP, Beuchle D, Furutani-Seiki M, Kelsh RN, Warga RM, Granato M, Haffter P, Hammerschmidt M, Kane DA, Mullins MC, Odenthal J, van Eeden FJ, Nusslein-Volhard C. Mutations affecting neurogenesis and brain morphology in the zebrafish, *Danio rerio*. *Development*. 1996; 123:205–216. [PubMed: 9007241]
- Kapoor TM, Mayer TU, Coughlin ML, Mitchison TJ. Probing spindle assembly mechanisms with monastrol, a small molecule inhibitor of the mitotic kinesin, Eg5. *J Cell Biol*. 2000; 150:975–988. [PubMed: 10973989]

- Kaprielian Z, Runko E, Imondi R. Axon guidance at the midline choice point. *Dev Dyn*. 2001; 221:154–181. [PubMed: 11376484]
- Karlstrom RO, Talbot WS, Schier AF. Comparative synteny cloning of zebrafish you-too: mutations in the Hedgehog target *gli2* affect ventral forebrain patterning. *Genes Dev*. 1999; 13:388–393. [PubMed: 10049354]
- Karlstrom RO, Trowe T, Klostermann S, Baier H, Brand M, Crawford AD, Grunewald B, Haffter P, Hoffmann H, Meyer SU, Muller BK, Richter S, van Eeden FJ, Nusslein-Volhard C, Bonhoeffer F. Zebrafish mutations affecting retinotectal axon pathfinding. *Development*. 1996; 123:427–438. [PubMed: 9007260]
- Kettenmann H, Verkhratsky A. Neuroglia: the 150 years after. *Trends Neurosci*. 2008; 31:653–659. [PubMed: 18945498]
- Kim H, Shin J, Kim S, Poling J, Park HC, Appel B. Notch-regulated oligodendrocyte specification from radial glia in the spinal cord of zebrafish embryos. *Dev Dyn*. 2008; 237:2081–2089. [PubMed: 18627107]
- Klambt C, Schimmelpfeng K, Hummel T. Glia development in the embryonic CNS of *Drosophila*. *Adv Exp Med Biol*. 1999; 468:23–32. [PubMed: 10635017]
- Klein E, DeBonis S, Thiede B, Skoufias DA, Kozielski F, Lebeau L. New chemical tools for investigating human mitotic kinesin Eg5. *Bioorg Med Chem*. 2007; 15:6474–6488. [PubMed: 17587586]
- Koo BK, Lim HS, Song R, Yoon MJ, Yoon KJ, Moon JS, Kim YW, Kwon MC, Yoo KW, Kong MP, Lee J, Chitnis AB, Kim CH, Kong YY. Mind bomb 1 is essential for generating functional Notch ligands to activate Notch. *Development*. 2005; 132:3459–3470. [PubMed: 16000382]
- Koo BK, Yoon MJ, Yoon KJ, Im SK, Kim YY, Kim CH, Suh PG, Jan YN, Kong YY. An obligatory role of mind bomb-1 in notch signaling of mammalian development. *PLoS One*. 2007; 2:e1221. [PubMed: 18043734]
- Kosan C, Kunz J. Identification and characterisation of the gene TWIST NEIGHBOR (TWISTNB) located in the microdeletion syndrome 7p21 region. *Cytogenet Genome Res*. 2002; 97:167–170. [PubMed: 12438708]
- Kriegstein A, Alvarez-Buylla A. The glial nature of embryonic and adult neural stem cells. *Annu Rev Neurosci*. 2009; 32:149–184. [PubMed: 19555289]
- Kucenas S, Takada N, Park HC, Woodruff E, Broadie K, Appel B. CNS-derived glia ensheath peripheral nerves and mediate motor root development. *Nat Neurosci*. 2008; 11:143–151. [PubMed: 18176560]
- Lai K, Amsterdam A, Farrington S, Bronson RT, Hopkins N, Lees JA. Many ribosomal protein mutations are associated with growth impairment and tumor predisposition in zebrafish. *Dev Dyn*. 2009; 238:76–85. [PubMed: 19097187]
- Lam CS, Marz M, Strahle U. *gfap* and *nestin* reporter lines reveal characteristics of neural progenitors in the adult zebrafish brain. *Dev Dyn*. 2009; 238:475–486. [PubMed: 19161226]
- Learte AR, Hidalgo A. The role of glial cells in axon guidance, fasciculation and targeting. *Adv Exp Med Biol*. 2007; 621:156–166. [PubMed: 18269218]
- Lee J, Gross JM. Laminin beta1 and gamma1 containing laminins are essential for basement membrane integrity in the zebrafish eye. *Invest Ophthalmol Vis Sci*. 2007; 48:2483–2490. [PubMed: 17525174]
- Lele Z, Folchert A, Concha M, Rauch GJ, Geisler R, Rosa F, Wilson SW, Hammerschmidt M, Bally-Cuif L. *parachute/n-cadherin* is required for morphogenesis and maintained integrity of the zebrafish neural tube. *Development*. 2002; 129:3281–3294. [PubMed: 12091300]
- Lindwall C, Fothergill T, Richards LJ. Commissure formation in the mammalian forebrain. *Curr Opin Neurobiol*. 2007; 17:3–14. [PubMed: 17275286]
- Liu Y, Pathak N, Kramer-Zucker A, Drummond IA. Notch signaling controls the differentiation of transporting epithelia and multiciliated cells in the zebrafish pronephros. *Development*. 2007; 134:1111–1122. [PubMed: 17287248]
- Lowery LA, De Rienzo G, Gutzman JH, Sive H. Characterization and classification of zebrafish brain morphology mutants. *Anat Rec (Hoboken)*. 2009; 292:94–106. [PubMed: 19051268]

- Lowery LA, Rubin J, Sive H. Whitesnake/sfpq is required for cell survival and neuronal development in the zebrafish. *Dev Dyn.* 2007; 236:1347–1357. [PubMed: 17393485]
- Lunde K, Belting HG, Driever W. Zebrafish pou5f1/pou2, homolog of mammalian Oct4, functions in the endoderm specification cascade. *Curr Biol.* 2004; 14:48–55. [PubMed: 14711414]
- Malicki J, Neuhauss SC, Schier AF, Solnica-Krezel L, Stemple DL, Stainier DY, Abdelilah S, Zwartkuis F, Rangini Z, Driever W. Mutations affecting development of the zebrafish retina. *Development.* 1996; 123:263–273. [PubMed: 9007246]
- Maliga Z, Kapoor TM, Mitchison TJ. Evidence that monastrol is an allosteric inhibitor of the mitotic kinesin Eg5. *Chem Biol.* 2002; 9:989–996. [PubMed: 12323373]
- Maliga Z, Mitchison TJ. Small-molecule and mutational analysis of allosteric Eg5 inhibition by monastrol. *BMC Chem Biol.* 2006; 6:2. [PubMed: 16504166]
- Marcus RC, Easter SS Jr. Expression of glial fibrillary acidic protein and its relation to tract formation in embryonic zebrafish (*Danio rerio*). *J Comp Neurol.* 1995; 359:365–381. [PubMed: 7499535]
- Marlow F, Gonzalez EM, Yin C, Rojo C, Solnica-Krezel L. No tail co-operates with non-canonical Wnt signaling to regulate posterior body morphogenesis in zebrafish. *Development.* 2004; 131:203–216. [PubMed: 14660439]
- Marthiens V, Gavard J, Lambert M, Mege RM. Cadherin-based cell adhesion in neuromuscular development. *Biol Cell.* 2002; 94:315–326. [PubMed: 12500939]
- Masai I, Lele Z, Yamaguchi M, Komori A, Nakata A, Nishiwaki Y, Wada H, Tanaka H, Nojima Y, Hammerschmidt M, Wilson SW, Okamoto H. N-cadherin mediates retinal lamination, maintenance of forebrain compartments and patterning of retinal neurites. *Development.* 2003; 130:2479–2494. [PubMed: 12702661]
- Mason CA, Sretavan DW. Glia, neurons, and axon pathfinding during optic chiasm development. *Curr Opin Neurobiol.* 1997; 7:647–653. [PubMed: 9384544]
- Mayer TU, Kapoor TM, Haggarty SJ, King RW, Schreiber SL, Mitchison TJ. Small molecule inhibitor of mitotic spindle bipolarity identified in a phenotype-based screen. *Science.* 1999; 286:971–974. [PubMed: 10542155]
- Miyamoto DT, Perlman ZE, Burbank KS, Groen AC, Mitchison TJ. The kinesin Eg5 drives poleward microtubule flux in *Xenopus laevis* egg extract spindles. *J Cell Biol.* 2004; 167:813–818. [PubMed: 15583027]
- Nissen RM, Amsterdam A, Hopkins N. A zebrafish screen for craniofacial mutants identifies wdr68 as a highly conserved gene required for endothelin-1 expression. *BMC Dev Biol.* 2006; 6:28. [PubMed: 16759393]
- Nona SN, Shehab SA, Stafford CA, Cronly-Dillon JR. Glial fibrillary acidic protein (GFAP) from goldfish: its localisation in visual pathway. *Glia.* 1989; 2:189–200. [PubMed: 2526081]
- Odenthal J, Haffter P, Vogelsang E, Brand M, van Eeden FJ, Furutani-Seiki M, Granato M, Hammerschmidt M, Heisenberg CP, Jiang YJ, Kane DA, Kelsh RN, Mullins MC, Warga RM, Allende ML, Weinberg ES, Nusslein-Volhard C. Mutations affecting the formation of the notochord in the zebrafish, *Danio rerio*. *Development.* 1996; 123:103–115. [PubMed: 9007233]
- Park HC, Appel B. Delta-Notch signaling regulates oligodendrocyte specification. *Development.* 2003; 130:3747–3755. [PubMed: 12835391]
- Parsons MJ, Pollard SM, Saude L, Feldman B, Coutinho P, Hirst EM, Stemple DL. Zebrafish mutants identify an essential role for laminins in notochord formation. *Development.* 2002; 129:3137–3146. [PubMed: 12070089]
- Paulus JD, Halloran MC. Zebrafish bashful/laminin-alpha 1 mutants exhibit multiple axon guidance defects. *Dev Dyn.* 2006; 235:213–224. [PubMed: 16261616]
- Pellet S, Tracy JW. Mak16p is required for the maturation of 25S and 5.8S rRNAs in the yeast *Saccharomyces cerevisiae*. *Yeast.* 2006; 23:495–506. [PubMed: 16710831]
- Perdew GH. Ah receptor binding to its cognate response element is required for dioxin-mediated toxicity. *Toxicol Sci.* 2008; 106:301–303. [PubMed: 18930947]
- Phi JH, Park SH, Chae JH, Hong KH, Park SS, Kang JH, Jun JK, Cho BK, Wang KC, Kim SK. Congenital subependymal giant cell astrocytoma: clinical considerations and expression of radial glial cell markers in giant cells. *Childs Nerv Syst.* 2008; 24:1499–1503. [PubMed: 18629509]

- Pogoda HM, Sternheim N, Lyons DA, Diamond B, Hawkins TA, Woods IG, Bhatt DH, Franzini-Armstrong C, Dominguez C, Arana N, Jacobs J, Nix R, Fetcho JR, Talbot WS. A genetic screen identifies genes essential for development of myelinated axons in zebrafish. *Dev Biol.* 2006; 298:118–131. [PubMed: 16875686]
- Powell EM, Geller HM. Dissection of astrocyte-mediated cues in neuronal guidance and process extension. *Glia.* 1999; 26:73–83. [PubMed: 10088674]
- Powell EM, Meiners S, DiProspero NA, Geller HM. Mechanisms of astrocyte-directed neurite guidance. *Cell Tissue Res.* 1997; 290:385–393. [PubMed: 9321702]
- Ramón y Cajal, S. *Histology of the Nervous System of Man and Vertebrates.* Oxford University Press; 1911.
- Raymond PA, Barthel LK, Bernardos RL, Perkowski JJ. Molecular characterization of retinal stem cells and their niches in adult zebrafish. *BMC Dev Biol.* 2006; 6:36. [PubMed: 16872490]
- Ruiz i Altaba A, Stecca B, Sanchez P. Hedgehog--Gli signaling in brain tumors: stem cells and paradevelopmental programs in cancer. *Cancer Lett.* 2004; 204:145–157. [PubMed: 15013214]
- Sadler KC, Amsterdam A, Soroka C, Boyer J, Hopkins N. A genetic screen in zebrafish identifies the mutants *vps18*, *nf2* and *foie gras* as models of liver disease. *Development.* 2005; 132:3561–3572. [PubMed: 16000385]
- Sanchez-Camacho C, Bovolenta P. Emerging mechanisms in morphogen-mediated axon guidance. *Bioessays.* 2009; 31:1013–1025. [PubMed: 19705365]
- Sann S, Wang Z, Brown H, Jin Y. Roles of endosomal trafficking in neurite outgrowth and guidance. *Trends Cell Biol.* 2009; 19:317–324. [PubMed: 19540123]
- Sarli V, Giannis A. Inhibitors of mitotic kinesins: next-generation antimicrotubule inhibitors. *ChemMedChem.* 2006; 1:293–298. [PubMed: 16892362]
- Sarli V, Huemmer S, Sunder-Plassmann N, Mayer TU, Giannis A. Synthesis and biological evaluation of novel EG5 inhibitors. *Chembiochem.* 2005; 6:2005–2013. [PubMed: 16216042]
- Sawin KE, LeGuellec K, Philippe M, Mitchison TJ. Mitotic spindle organization by a plus-end-directed microtubule motor. *Nature.* 1992; 359:540–543. [PubMed: 1406972]
- Sawin KE, Mitchison TJ. Mutations in the kinesin-like protein Eg5 disrupting localization to the mitotic spindle. *Proc Natl Acad Sci U S A.* 1995; 92:4289–4293. [PubMed: 7753799]
- Schauerte HE, van Eeden FJ, Fricke C, Odenthal J, Strahle U, Haffter P. Sonic hedgehog is not required for the induction of medial floor plate cells in the zebrafish. *Development.* 1998; 125:2983–2993. [PubMed: 9655820]
- Schier AF, Neuhauss SC, Harvey M, Malicki J, Solnica-Krezel L, Stainier DY, Zwartkuis F, Abdelilah S, Stemple DL, Rangini Z, Yang H, Driever W. Mutations affecting the development of the embryonic zebrafish brain. *Development.* 1996; 123:165–178. [PubMed: 9007238]
- Shaham S. Glia-neuron interactions in nervous system function and development. *Curr Top Dev Biol.* 2005; 69:39–66. [PubMed: 16243596]
- Shin J, Poling J, Park HC, Appel B. Notch signaling regulates neural precursor allocation and binary neuronal fate decisions in zebrafish. *Development.* 2007; 134:1911–1920. [PubMed: 17442701]
- Shu T, Butz KG, Plachez C, Gronostajski RM, Richards LJ. Abnormal development of forebrain midline glia and commissural projections in *Nfia* knock-out mice. *J Neurosci.* 2003a; 23:203–212. [PubMed: 12514217]
- Shu T, Puche AC, Richards LJ. Development of midline glial populations at the corticoseptal boundary. *J Neurobiol.* 2003b; 57:81–94. [PubMed: 12973830]
- Song R, Kim YW, Koo BK, Jeong HW, Yoon MJ, Yoon KJ, Jun DJ, Im SK, Shin J, Kong MP, Kim KT, Yoon K, Kong YY. *Mind bomb 1* in the lymphopoietic niches is essential for T and marginal zone B cell development. *J Exp Med.* 2008; 205:2525–2536. [PubMed: 18824586]
- Stuermer CA. Retinotopic organization of the developing retinotectal projection in the zebrafish embryo. *J Neurosci.* 1988; 8:4513–4530. [PubMed: 2848935]
- Sun Z, Amsterdam A, Pazour GJ, Cole DG, Miller MS, Hopkins N. A genetic screen in zebrafish identifies cilia genes as a principal cause of cystic kidney. *Development.* 2004; 131:4085–4093. [PubMed: 15269167]



- Sun Z, Hopkins N. *vhnf1*, the *MODY5* and familial GCKD-associated gene, regulates regional specification of the zebrafish gut, pronephros, and hindbrain. *Genes Dev.* 2001; 15:3217–3229. [PubMed: 11731484]
- Suzuki SC, Takeichi M. Cadherins in neuronal morphogenesis and function. *Dev Growth Differ.* 2008; 50(Suppl 1):S119–130. [PubMed: 18430170]
- Taber KH, Hurley RA. Astroglia: not just glue. *J Neuropsychiatry Clin Neurosci.* 2008; 20:iv–129.
- Tawk M, Araya C, Lyons DA, Reugels AM, Girdler GC, Bayley PR, Hyde DR, Tada M, Clarke JD. A mirror-symmetric cell division that orchestrates neuroepithelial morphogenesis. *Nature.* 2007; 446:797–800. [PubMed: 17392791]
- Thiery JP. Cell adhesion in development: a complex signaling network. *Curr Opin Genet Dev.* 2003; 13:365–371. [PubMed: 12888009]
- Tokumoto M, Gong Z, Tsubokawa T, Hew CL, Uyemura K, Hotta Y, Okamoto H. Molecular heterogeneity among primary motoneurons and within myotomes revealed by the differential mRNA expression of novel *islet-1* homologs in embryonic zebrafish. *Dev Biol.* 1995; 171:578–589. [PubMed: 7556938]
- Tomaselli KJ, Neugebauer KM, Bixby JL, Lilien J, Reichardt LF. N-cadherin and integrins: two receptor systems that mediate neuronal process outgrowth on astrocyte surfaces. *Neuron.* 1988; 1:33–43. [PubMed: 2856086]
- Trevarrow B, Marks DL, Kimmel CB. Organization of hindbrain segments in the zebrafish embryo. *Neuron.* 1990; 4:669–679. [PubMed: 2344406]
- Trowe T, Klostermann S, Baier H, Granato M, Crawford AD, Grunewald B, Hoffmann H, Karlstrom RO, Meyer SU, Muller B, Richter S, Nusslein-Volhard C, Bonhoeffer F. Mutations disrupting the ordering and topographic mapping of axons in the retinotectal projection of the zebrafish, *Danio rerio*. *Development.* 1996; 123:439–450. [PubMed: 9007261]
- Valentine MT, Fordyce PM, Block SM. Eg5 steps it up! *Cell Div.* 2006a; 1:31. [PubMed: 17173688]
- Valentine MT, Fordyce PM, Krzysiak TC, Gilbert SP, Block SM. Individual dimers of the mitotic kinesin motor Eg5 step processively and support substantial loads in vitro. *Nat Cell Biol.* 2006b; 8:470–476. [PubMed: 16604065]
- van der Lelij P, Godthelp BC, van Zon W, van Gosliga D, Oostra AB, Steltenpool J, de Groot J, Scheper RJ, Wolthuis RM, Waisfisz Q, Darroudi F, Joenje H, de Winter JP. The cellular phenotype of Roberts syndrome fibroblasts as revealed by ectopic expression of *ESCO2*. *PLoS One.* 2009; 4:e6936. [PubMed: 19738907]
- Varga ZM, Amores A, Lewis KE, Yan YL, Postlethwait JH, Eisen JS, Westerfield M. Zebrafish smoothed functions in ventral neural tube specification and axon tract formation. *Development.* 2001; 128:3497–3509. [PubMed: 11566855]
- Vega H, Waisfisz Q, Gordillo M, Sakai N, Yanagihara I, Yamada M, van Gosliga D, Kayserili H, Xu C, Ozono K, Jabs EW, Inui K, Joenje H. Roberts syndrome is caused by mutations in *ESCO2*, a human homolog of yeast *ECO1* that is essential for the establishment of sister chromatid cohesion. *Nat Genet.* 2005; 37:468–470. [PubMed: 15821733]
- Wechsler-Reya RSM. The developmental biology of brain tumors. *Annu Rev Neurosci.* 2001; 24:385–428. [PubMed: 11283316]
- Wei X, Malicki J. *nagie oko*, encoding a MAGUK-family protein, is essential for cellular patterning of the retina. *Nat Genet.* 2002; 31:150–157. [PubMed: 11992120]
- Wei X, Zou J, Takechi M, Kawamura S, Li L. *Nok* plays an essential role in maintaining the integrity of the outer nuclear layer in the zebrafish retina. *Exp Eye Res.* 2006; 83:31–44. [PubMed: 16530752]
- Westerfield, M. *The Zebrafish Book, A guide for the laboratory use of zebrafish (Danio rerio)*. University of Oregon Press; Eugene: 2007.
- Westfall TA, Brimeyer R, Twedt J, Gladon J, Olberding A, Furutani-Seiki M, Slusarski DC. *Wnt-5/* pipetail functions in vertebrate axis formation as a negative regulator of *Wnt/beta-catenin* activity. *J Cell Biol.* 2003; 162:889–898. [PubMed: 12952939]
- Wickner RB. Host function of *MAK16*: G1 arrest by a *mak16* mutant of *Saccharomyces cerevisiae*. *Proc Natl Acad Sci U S A.* 1988; 85:6007–6011. [PubMed: 3045810]

- Wiellette EL, Sive H. *vhnf1* and *Fgf* signals synergize to specify rhombomere identity in the zebrafish hindbrain. *Development*. 2003; 130:3821–3829. [PubMed: 12835397]
- Wilson SW, Ross LS, Parrett T, Easter SS Jr. The development of a simple scaffold of axon tracts in the brain of the embryonic zebrafish, *Brachydanio rerio*. *Development*. 1990; 108:121–145. [PubMed: 2351059]
- Yamagata K, Nammo T, Moriwaki M, Ihara A, Iizuka K, Yang Q, Satoh T, Li M, Uenaka R, Okita K, Iwahashi H, Zhu Q, Cao Y, Imagawa A, Tochino Y, Hanafusa T, Miyagawa J, Matsuzawa Y. Overexpression of dominant-negative mutant hepatocyte nuclear factor-1 alpha in pancreatic beta-cells causes abnormal islet architecture with decreased expression of E-cadherin, reduced beta-cell proliferation, and diabetes. *Diabetes*. 2002; 51:114–123. [PubMed: 11756330]
- Yang X, Zou J, Hyde DR, Davidson LA, Wei X. Stepwise maturation of apicobasal polarity of the neuroepithelium is essential for vertebrate neurulation. *J Neurosci*. 2009; 29:11426–11440. [PubMed: 19759292]
- Yeo SY. Zebrafish CiA interneurons are late-born primary neurons. *Neurosci Lett*. 2009; 466:131–134. [PubMed: 19800937]
- Yoo KW, Kim EH, Jung SH, Rhee M, Koo BK, Yoon KJ, Kong YY, Kim CH. *Snx5*, as a Mind bomb-binding protein, is expressed in hematopoietic and endothelial precursor cells in zebrafish. *FEBS Lett*. 2006; 580:4409–4416. [PubMed: 16857196]
- Zou J, Lathrop KL, Sun M, Wei X. Intact retinal pigment epithelium maintained by *Nok* is essential for retinal epithelial polarity and cellular patterning in zebrafish. *J Neurosci*. 2008; 28:13684–13695. [PubMed: 19074041]

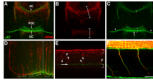


**Figure 1. Wild type axon and astroglial morphology**

(A-F) Fluorescent immunolabeling of axons ( $\alpha$ AT, green) and astroglial cells ( $\alpha$ Gfap, red) in a 40hpf wild type embryo. (A-C) Ventral view of the forebrain, anterior up; eyes out of view on sides. (A) Combined red and green channels show the association of the forebrain commissures with glial bridges. The anterior commissure forms in the telencephalon and the post optic commissure and optic chiasm form in the diencephalon, which are separated by the optic recess. (B) Gfap expressing astroglia are condensed into two “bridges”, one in the telencephalon (upper bracket) and one in the diencephalon (lower bracket) (Barresi et al., 2005). (C) There are three axonal pathways in the forebrain: the postoptic commissure (lower bracket), anterior commissure (upper bracket), and the optic nerves (arrowheads) that cross the midline to form the optic chiasm (arrow). (D) Lateral view of the hindbrain, anterior left, dorsal up. Long radial glial processes are segmentally arranged (brackets) and span from the ventral to dorsal axis of the hindbrain (bracket). (E) Lateral view of the spinal cord. This image is focused on the midline/ventricular zone of the spinal cord, with the roofplate to the top and floorplate to the bottom (brackets). Radial glial cell bodies (red, arrowheads) and cilia (green, arrow) are visible just above the floorplate. (F) Lateral view of motor nerves in the trunk, anterior left, dorsal up. Axon labeling (green) is distinct from labeling of motor axon associated glia (red).  $\alpha$ AT (anti-Acetylated Tubulin),  $\alpha$ Gfap (anti-Glial fibrillary acidic protein), tel (telencephalon), di (diencephalon), POC (postoptic commissure), AC (anterior commissure), optic chiasm (OC). Scale bar = 50 $\mu$ m.

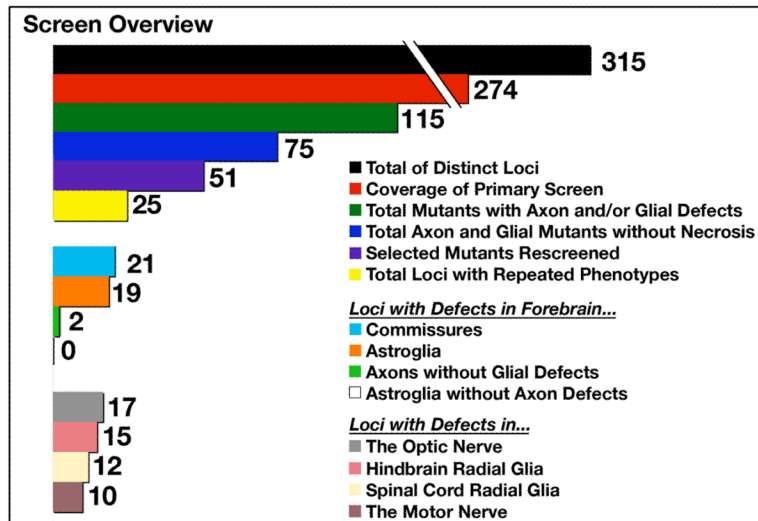


**Figure 2. Overview of screen results**

Numbers represent individual genes identified for each category described in the color key. Twenty-five distinct loci were identified that affect axonal anatomy and/or astroglial pattern. Astroglial defects in the forebrain were always correlated with axonal defects.

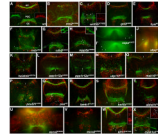


### Figure 3. Forebrain mutants

(A-X) Ventral views of zebrafish forebrains showing axons ( $\alpha$ AT, green) and astroglial cells ( $\alpha$ Gfap, red). Anterior is up. (A) WT forebrain commissures. Insets show POC (left) and the corresponding glial bridge (right) as single channels. Commissures and the optic chiasm all cross at the midline as cohesive bundles in direct association with glial bridges. (B-X) Mutants with defects in forebrain astroglia and/or axonal anatomy. (B) *rrm2* mutants, known to have widespread necrosis, display severe astroglial reductions and dramatic optic nerve and commissural axon phenotypes including reductions and pathfinding errors. Mutants that had reduced or absent optic nerves include; (C) *wnt5b*, (D) *gnl3*, (E) *bysl*, (K) *twistnb*, (L,M) *ppp1r12a*, (N) *utp111*, (O) *mak16*, (P) *pou5f1*, (Q) *pes*, (R) *lamb1*, (S) *hnf1b*, (T) *abhd11*, (U,V) *esco2*, and (W) *kif11*. Optic nerves were defasciculated in; (G) *cdh2*, (H) *mpp5a*, and (I) *copa* mutants. RGC axons made pathfinding errors in; (J) *sfpq*, (L) *ppp1r12a*, and (C) *wnt5b* mutants. Mutants having defasciculated commissures and/or axon pathfinding errors were; (C) *wnt5b*, (G) *cdh2*, (H) *mpp5a*, (L,M) *ppp1r12a*, (O) *mak16*, (P) *pou5f1*, (Q) *pes*, (R) *lamb1*, (S) *hnf1b*, (T) *abhd11*, (W) *kif11*, and (X) *csnk1a1*. The only mutants that did not exhibit astroglial patterning defects were (E) *bysl*, (G) *cdh2*, and (S) *hnf1b*. Insets show enlargements of boxed regions in the corresponding images. Arrows indicate mislocated axons phenotypes in the AC, POC (C,F,K-O), or optic nerves (S). Arrowheads highlight locations of specific axonal pathfinding errors (C,H-J,Q-T,W), astroglial defects (X), or the beginning of the optic nerves (F). White dots denote location of ectopic astroglial cell bodies at the forebrain ventricular zone (W, inset).



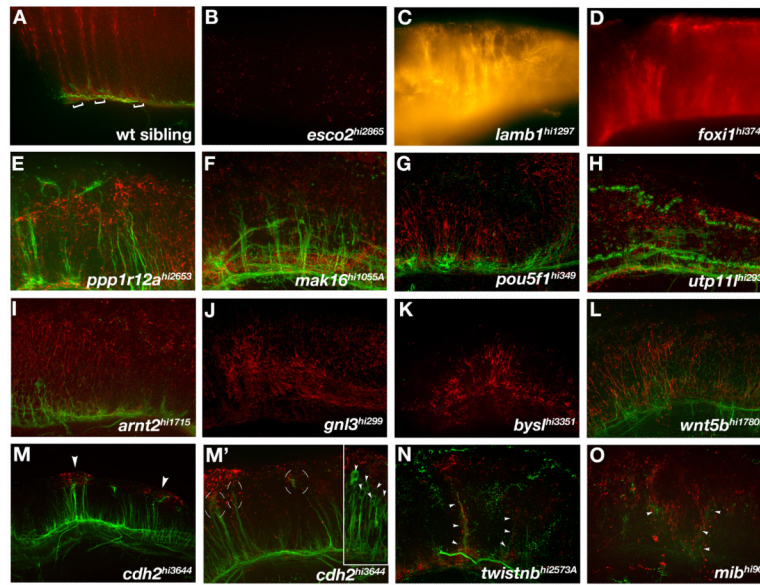


#### Figure 4. Hindbrain mutants

(A-O) Lateral views of hindbrains of (A) wild type and (B-O) mutant embryos. (A) Brackets show the segmental organization of radial glial cells that extend processes dorsally to the pial surface. (B) *esco2* mutants had reduced radial glia in the hindbrain radial. (C-G) *lamb1*, *foxi*, *ppp1r12a*, *mak16*, and *pou5f1* mutants had disorganized radial glial process that were still segmentally organized. (H-L) *utp11l*, *arnt2*, *gnl3*, *bysl*, and *wnt5b* mutants also had disorganized radial glial processes in a generally disrupted hindbrain. (M-O) *cdh2*, *twistnb*, and *mib* mutants had ectopic clusters of Gfap labeling. (M) *cdh2* mutants showed ectopic dorsal glial clusters (M, arrowheads) associated with mis-located axonal projections (M', circular brackets). (M') Inset shows another *cdh2* mutant embryo with neuronal cell bodies associated with glial clusters (arrowheads). (N,O) *twistnb* and *mib* mutants had mispositioned axons associated with mispatterned astroglia (arrowheads). (B,C,D,J,K) Axon labeling is not visible due to faint fluorescent labeling.

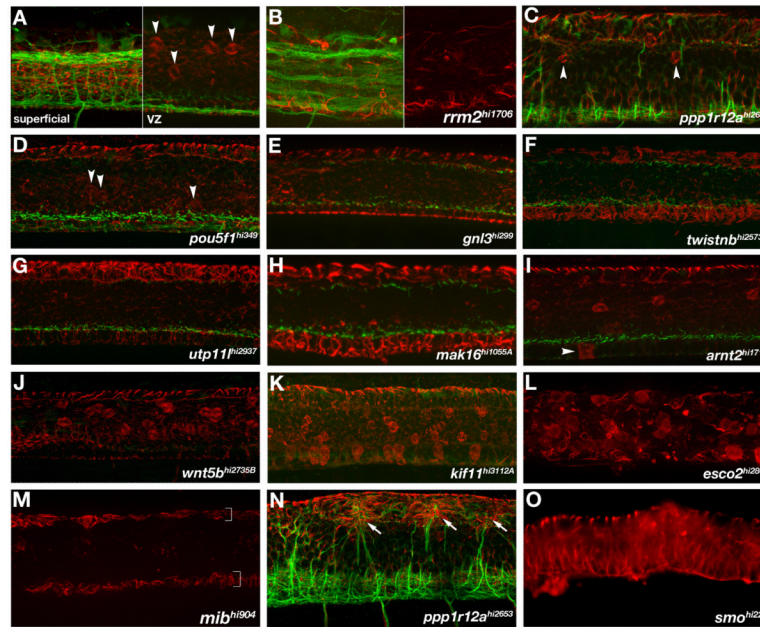


### Figure 5. Spinal cord radial glial mutants

(A-O) Lateral views of the trunk, anterior left. (A) Wild type spinal cord showing axon bundles (green) and radial glia (red) observed in a full maximum intensity projection (superficial, left panel). The typical placement and number of Gfap labeled radial glial cell bodies at the ventricular zone (arrowheads) is seen in a projection of optical slices encompassing the full ventricular zone (“VZ”, right panel). (B) *rrm2* mutants had axonal and astroglial phenotypes characteristic of non-specific defects that are likely caused by ubiquitous cell death. Right half shows only the channel for  $\alpha$ Gfap labeling (red), while the left half also includes  $\alpha$ AT labeling for axons. (C-O) Mutants with altered numbers of  $\alpha$ Gfap labeled cell bodies within the spinal cord. (C,D) *ppp1r12a* and *pou5f1* mutants had reduced numbers of  $\alpha$ Gfap labeled cell bodies (arrowheads) near the ventricular zone (A; see also Fig. 1E). (E-H) *gnl3*, *twistnb*, *utp11* and *mak16* mutants had no  $\alpha$ Gfap labeled cell bodies in the ventricular zone. (I-L) In contrast, *arnt2* mutants had ectopic Gfap+ cell bodies in the floorplate (I), and *wnt5b*, *kif1*, and *esco2* mutants had increased numbers of Gfap+ cell bodies in the ventricular zone (J-L). (M-O) *mib*, *ppp1r12a*, and *smo* mutants all had fewer or no  $\alpha$ Gfap labeled cell bodies and radial glial processes. *mib* mutants had no radial glial processes except in the regions of the roof- and floorplates (M, brackets). (N) In *ppp1r12a* mutants, aberrant axon projections were associated with ectopic dorsal clusters of radial processes (arrows). (O) *smoothened* mutants had no  $\alpha$ Gfap labeled cell bodies and generally disorganized radial glial processes.

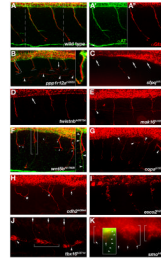


### Figure 6. Motor nerve mutants

(A-K) Lateral view the trunk labeled showing motor axons (green) and motor axon associated glia (red). Anterior left, dorsal up. Confocal z-stacks span the region from the spinal cord exit point to the most superficial location of the spinal nerve. For technical reasons, axon labeling was only successful in *ppp1r12a*, *wnt5b<sup>hi1780B</sup>*, and *smo* mutants. All other mutants descriptions are based solely on  $\alpha$ Gfap labeling of motor axon associated glia. (A) Wild type spinal nerves in two full trunk segments. (A', A'') Individual axonal (green) and glial (red) labeling corresponding to the region in A between dashed lines. (B) In *ppp1r12a* mutants motor axons and associated glia terminate (dashed lines) before reaching the lateral line (arrowheads). Motor axons (green) and glial processes (red) are tightly associated (bracket, inset). A mis-localized glial process is seen in one segment (arrow). (C-E) *sfpq*, *twistnb*, and *mak16* mutants had truncated (arrowheads) or absent (arrows) motor axon associated glia. (F, G) *wnt5b* and *copa* mutants had excessively branched (arrowheads) motor axon associated glia. In some cases motor axons projected correctly (F, brackets, inset, arrowheads), while the associated glia were truncated and disorganized (F, G, arrowheads). (H) *cdh2* mutants had errors in the positioning of motor axon associated glia akin to motor axon wandering (asterisks), excessive branching (arrowhead) and variable truncations (arrow). (I) *esco2* mutants had reduced and fragmented motor axon associated glia. (J) *tbx16* mutants had ectopic glia located ventrally (arrowheads). In some somites glia spanned somite boundaries (bracket). (K) *smo* mutants had ectopic glial clusters (brackets) with aberrant projections (arrows). An overlaid inset shows an over-intensified image of  $\alpha$ AT labeling to make visible the rare case in which a motor axon (arrowheads) is not associated with ectopic  $\alpha$ Gfap labeled cell clusters (arrow).

Table 1

## List of insertional mutants and their associated phenotypes

Gene Symbol	Gene Name	Allele	Phenotypes exhibited									
			Forebrain			Hindbrain		Spinal Cord				
			CA	ON	Astroglia	Radial Glia	Axons	Radial Glia	MN			
<i>abhd11*</i>	<i>abhydrolase domain containing 11</i>	hi3305	X	X	X							
<i>arn2</i>	<i>aryl hydrocarbon receptor nuclear translocator 2</i>	hi1715	X		X	X	X	X			X	
<i>byst1*</i>	<i>bystin-like</i>	hi3351		X		X						
<i>cdh2*</i>	<i>cadherin 2, neuronal</i>	hi3644/hi1389	X	X		X	X	X				X
<i>chd*</i>	<i>chordin</i>	hi2293	X	X		X						
<i>copa*</i>	<i>coatamer protein complex, subunit alpha</i>	hi1872		X								X
<i>csnk1a1</i>	<i>casein kinase 1, alpha 1</i>	hi2069	X			X						
<i>esco2*</i>	<i>establishment of cohesion 1 homolog 2</i>	hi2865	X	X		X	X	X			X	X
<i>foxi1*</i>	<i>forkhead box 11</i>	hi3747					X					
<i>gnl3</i>	<i>guanine nucleotide binding protein-like 3 (nuclear)</i>	hi299	X	X		X	X	X			X	
<i>hnflb*</i>	<i>HNF1 homeobox b</i>	hi1843	X	X								
<i>kif11*</i>	<i>kinesin family member 11</i>	hi3112A	X			X					X	
<i>lamb1*</i>	<i>laminin, beta 1</i>	hi1297	X	X		X	X					
<i>mak16*</i>	<i>MAK16 homolog (S. cerevisiae)</i>	hi1055A	X			X	X	X			X	X
<i>mib*</i>	<i>mind bomb</i>	hi904	X	X		X	X	X			X	
<i>mpps5a*</i>	<i>membrane protein, palmitoylated 5a (MAGUK p55 subfamily member 5a)</i>	hi2226	X	X		X						
<i>pes</i>	<i>pescadillo</i>	hi2	X	X		X						
<i>pou5f1*</i>	<i>POU domain, class 5, transcription factor 1</i>	hi349/hi1940	X	X		X	X	X			X	
<i>ppp1r12a*</i>	<i>protein phosphatase 1, regulatory (inhibitor) subunit 12A</i>	hi2653	X	X		X	X	X			X	X
<i>sfpq*</i>	<i>splicing factor proline/glutamine rich (polypyrimidine tract binding</i>	hi1779	X	X		X						X

Gene Symbol	Gene Name	Allele	Phenotypes exhibited										
			Forebrain			Hindbrain			Spinal Cord				
			CA	ON	Astroglia	Radial Glia	Axons	Radial Glia	MN				
<i>smo*</i>	<i>protein associated</i>												
<i>tbx16*</i>	<i>smoothed</i>	hi229	X	X	X	X	X	X	X	X	X	X	X
<i>twistnb*</i>	<i>T-box gene 16</i>	hi3714											X
<i>utp111*</i>	<i>TWIST neighbor</i>	hi2573A	X		X	X	X	X	X	X	X	X	X
<i>wnt5b*</i>	<i>UTP11-like, U3 small nucleolar ribonucleoprotein (yeast)</i>	hi2937	X		X	X	X	X	X	X	X	X	X
<i>wnt5b</i>	<i>wingless-type MMTV integration site family, member 5b</i>	hi1780B	X	X	X	X	X	X	X	X	X	X	X
<i>wnt5b</i>	<i>wingless-type MMTV integration site family, member 5b</i>	hi2735B	X		X							X	

Two alleles shown together indicate that both alleles were screened and had identical phenotypes. Commissural Axons (CA); Optic Nerve (ON); Motor Nerve (MN). Asterisks indicate a visible morphological abnormality by 48h (Amsterdam et al., 2004). See <http://web.mit.edu/hopkins/> for a detailed description of these morphological defects and references to mutants previously identified in other genetic screens.